Comparison of [11C]-(*R*)-PK 11195 and [11C]PBR28, Two Radioligands for Translocator Protein (18 kDa) in Human and Monkey: Implications for Positron Emission Tomographic Imaging of this Inflammation Biomarker

William C. Kreisl, MD[1], **Masahiro Fujita, MD, PhD**[1], **Yota Fujimura, PhD**[1,3], **Nobuyo Kimura, MD, PhD**[1], **Kimberly J. Jenko, MS**[1], **Pavitra Kannan, BA**[1], **Jinsoo Hong, MS**[1], **Cheryl L. Morse, MS**[1], **Sami S. Zoghbi, PhD**[1], **Robert L. Gladding**[1], **Steven Jacobson, PhD**[2], **Unsong Oh, MD**[2], **Victor W. Pike, PhD**[1], and **Robert B. Innis, MD, PhD**[1]

[1]Molecular Imaging Branch, National Institute of Mental Health, Bethesda, MD, USA

[2]Neuroimmunology Branch, National Institute of Neurological Disorders and Stroke, Bethesda, MD, USA

[3]Department of Psychiatry, School of Medicine, Teikyo University, Tokyo, Japan

Abstract

Ten percent of humans lack specific binding of [11C]PBR28 to 18 kDa translocator protein (TSPO), a biomarker for inflammation. "Non-binders" have not been reported using another TSPO radioligand, [11C]-(*R*)-PK 11195, despite its use for more than two decades. This study asked two questions: 1) What is the cause of non-binding to PBR28? 2) Why has this phenomenon not been reported using [11C]-(*R*)-PK 11195?

Methods—Five binders and five non-binders received whole-body imaging with both [11C]-(*R*)-PK 11195 and [11C]PBR28. *In vitro* binding was performed using leukocyte membranes from binders and non-binders and the tritiated versions of the ligand. Rhesus monkeys were imaged with [11C]-(*R*)-PK 11195 at baseline and after blockade of TSPOs.

Results—Using [11C]PBR28, uptake in all five organs with high densities of TSPO (lung, heart, brain, kidney, and spleen) was 50% to 75% lower in non-binders than in binders. In contrast, [11C]-(*R*)-PK 11195 distinguished binders and non-binders in only heart and lung. For the *in vitro* assay, [3H]PBR28 had more than ten-fold lower affinity to TSPO in non-binders than in binders. The *in vivo* specific binding of [11C]-(*R*)-PK 11195 in monkey brain was ~80-fold lower than that reported for [11C]PBR28.

Conclusions—Based on binding of [3H]PK 11195 to leukocyte membranes, both binders and non-binders express TSPO. Non-binding to PBR28 is caused by its low affinity for TSPO in non-binders. Non-binding may be differentially expressed in organs of the body. The relatively low *in vivo* specific binding of [11C]-(*R*)-PK 11195 may have obscured its detection of non-binding in peripheral organs.

Keywords

translocator protein (18 kDa); [11C]-(R)-PK 11195; [11C]PBR28; positron emission tomography

INTRODUCTION

Translocator protein (18-kDa) (TSPO) is highly expressed in the mitochondria of phagocytic inflammatory cells, including reactive astrocytes and activated microglia in brain (Papadopoulos et al., 2006). Because of high expression in these cells, positron emission tomographic (PET) imaging of TSPO, formerly called the peripheral benzodiazepine receptor, can localize inflammation in brain. For example, the TSPO-selective PET radioligand [11C]-(R)-PK 11195 has been used for more than two decades to identify areas of brain inflammation in several neurological diseases (for review, see Cagnin et al., 2007). Unfortunately, [11C]-(R)-PK 11195 seems to have a low ratio of "signal to noise" - *i.e.*, a low ratio of specific to nonspecific binding. Measured without correction for peripheral clearance, only about 50% of [11C]-(R)-PK 11195 uptake in monkey brain is specific (i.e., displaceable) (Petit-Taboue et al., 1991).

We recently developed what appeared to be an improved radioligand, [11C]PBR28, to image TSPO (Briard et al., 2008). More than 90% of [11C]PBR28 uptake in monkey brain is specific (Imaizumi et al., 2008). Although [11C]PBR28 appears much better than [11C]-(R)-PK 11195 to image TSPO in monkey brain, their relative merits in human subjects are unclear, in part because about 10% of human subjects paradoxically show no binding to [11C]PBR28. In about 90 human subjects studied to date, nine subjects (six healthy volunteers, two patients with multiple sclerosis, and one patient with HIV-associated neurocognitive disorder) behaved as if [11C]PBR28 were unable to bind to TSPO in brain and in peripheral organs (Brown et al., 2007; Fujita et al., 2008). In contrast, non-binding to TSPO has never been reported with [11C]-(R)-PK 11195, despite its use for more than two decades.

In this study, we sought to answer two questions: 1) What is the cause of non-binding to PBR28? and 2) Why has this phenomenon not previously been reported using [11C]-(R)-PK 11195? To answer these questions, we performed four different experiments. First, to determine whether non-binding is unique to [11C]PBR28, we scanned five binders and five non-binders with both radioligands: [11C]PBR28 and [11C]-(R)-PK 11195. Second, to determine whether non-binding is caused by a lack of expression of the TSPO protein, we measured *in vitro* binding of [3H]PK 11195 and [3H]PBR28 in an easily obtained human tissue, the cell membrane of peripheral leukocytes from both binders and non-binders. Third, the phenomenon of non-binding may have been overlooked with [11C]-(R)-PK 11195 because this radioligand has a low ratio of specific to nonspecific binding in brain. Since prior studies did not fully quantify brain uptake by correcting for peripheral clearance, we performed PET scanning in monkeys and also measured the concentration in arterial plasma of [11C]-(R)-PK 11195, at baseline and after receptor-saturating doses of non-radioactive TSPO ligand. Fourth, low specific binding of [11C]-(R)-PK 11195 might be caused by efflux transporters (including P-glycoprotein) at the blood-brain barrier that block the entry of radioligand. Rather than having low specific binding, the radioligand might simply be excluded from the brain. To answer this last question, we determined whether PK 11195 or PBR28 is a substrate for the three most prevalent efflux transporters at the blood-brain barrier.

METHODS

Radioligand synthesis

$[^{11}C]$-(R)-PK 11195 was synthesized by the $[^{11}C]$methylation of the desmethyl analogue using $[^{11}C]$iodomethane, which was prepared from cyclotron-produced $[^{11}C]$carbon dioxide. $[^{11}C]$-(R)-PK 11195 was then purified with reverse phase HPLC. Synthesis was performed in accordance with Investigational New Drug Application #101,908. $[^{11}C]$-(R)-PK 11195 was synthesized with high radiochemical purity (>98%) and specific activity at time of injection of 98 ± 34 GBq/µmol.

$[^{11}C]$PBR28 was synthesized according to previously published methods (Briard et al., 2008). Synthesis was performed in accordance with Investigational New Drug Application #76,441. A copy of the application is available at: http://pdsp.med.unc.edu/snidd/. $[^{11}C]$PBR28 was synthesized with high radiochemical purity (>99%) and had specific activity at time of injection of 122 ± 50 GBq/µmol.

Human whole-body study

Subject selection—Ten healthy volunteers (five female, five male) ages 33 ± 10 years were included in this study. Subjects underwent detailed medical history, physical exam, laboratory tests and electrocardiogram to exclude serious medical conditions, pregnancy, or illicit drug use. Whole-body PET imaging with $[^{11}C]$PBR28 was used to determine if subjects were binders or non-binders. Preliminary determination on binders or non-binders was performed based on the ratio of brain uptake at 13 minutes to peak brain uptake. A ratio of 60% or less was criteria for non-binding. One binder and four non-binders were previously identified in earlier studies (Brown et al., 2007; Fujita et al., 2008). The remaining five subjects were identified as binders or non-binders during the course of this study.

Image acquisition—All subjects underwent whole-body PET imaging with both $[^{11}C]$-(R)-PK 11195 and $[^{11}C]$PBR28. If a subject had been previously scanned with $[^{11}C]$PBR28 (Brown et al., 2007; Fujita et al., 2008), those images were used and the $[^{11}C]$PBR28 scan was not repeated. 2D dynamic images were acquired using a GE Advance tomograph (GE Medical Systems, Waukesha, WI) in 7 segments of the body (head to upper thigh) in frames of increasing duration (15 s to 4 min) for a total scan time of either 60 min (11 frames) or 120 min (14 frames). A 28-minute ^{68}Ge transmission scan was performed for attenuation correction prior to radioligand injection. Dynamic emission scans were acquired after intravenous bolus injection of 552 ± 158 MBq $[^{11}C]$-(R)-PK 11195 or 624 ± 166 MBq $[^{11}C]$PBR28.

Image analysis—On reconstructed whole-body images, organs known to express moderate to high levels of TSPO were identified using an organ-specific method as follows. Brain and kidney: regions of interest were manually drawn in a slice-by-slice manner on the tomographic images in the coronal plane. Lung and heart: tomographic images containing the organ were compressed into a single planar image in the axial plane and a region of interest was drawn over the organ. Spleen: tomographic images containing the organ were compressed into a single planar image in the coronal plane and a region of interest was drawn over the organ.

For each whole-body scan, recovery of radioactivity was calculated by placing a large region of interest over each bed position at each time frame. In two of the whole-body scans, moderate amounts of radioactivity were visibly apparent at the site of radioligand injection. The values of these pixels were set to zero before calculating the percent recovery of radioactivity for these scans.

The concentration of radioactivity in each organ was corrected for body weight, injected dose of radioligand, and percent recovery of radioactivity to obtain standardized uptake values (SUV). Time-activity curves were created for each organ by plotting SUV *vs*. time. The area under the time-activity curve from 5 to 20 minutes was used to measure uptake of radioligand in each organ. This time period was used because it better reflects receptor binding than the initial 5 min period, which is strongly affected by blood flow. By excluding the data after 20 minutes, we decreased the contamination of organ uptake by the build-up of radioactive metabolites.

Statistical analysis—Differences in the area under the time-activity curve from 5 to 20 minutes of each organ (brain, heart, lung, kidney, and spleen) were compared between human binders and non-binders by independent samples t-test using SPSS Statistics 17.0. Correction for multiple comparisons was performed using the false discovery rate (Benjamin and Hochberg, 1995), with threshold set at 0.05.

In vitro binding to membranes of human leukocytes

We obtained leukocytes (white blood cells) from a total of ten binders and eight non-binders, identified on the basis of brain imaging with [11C]PBR28 and using the criteria listed above. Leukocytes were chosen for this in vitro binding experiment because these cells are known to express TSPO (Moingeon et al., 1984) and are easily obtained from human subjects via phlebotomy. The binders were all healthy subjects, 5 males, and 5 females, 29 ± 7.6 years of age. The non-binders included 6 healthy subjects and 2 patients with multiple sclerosis. We could not distinguish patients and healthy subjects based on whole body imaging and *in vitro* binding. Thus, these two groups were combined as "non-binders" to increase the sample size. These non-binders had 6 males and 2 females, 31 ± 6.3 years of age.

Leukocytes were isolated from 200 mL heparinized whole blood by Ficoll-Hypaque density centrifugation using Lymphocyte Separation Medium (Lonza, Walkersville, MD), according to the manufacturer's instructions. Following isolation, these leukocytes were viably cryopreserved. Prior to the day of assay, the cells were thawed, diluted with an equal volume of buffer (50 mM HEPES, pH 7.4), homogenized with a Teflon pestle, and centrifuged at $20,000 \times g$ for 15 min at 4 °C. The resulting crude membrane pellet was resuspended in 2.4 mL buffer and stored at −70 °C. Protein concentration was determined using the Bradford Protein Assay (Bio-Rad, Hercules, CA).

Receptor binding followed procedures described by Ferrarese and colleagues (Ferrarese et al., 1990). The racemic radioligand [3H]PK 11195 (83.4 Ci/ mmol) was acquired from Perkin Elmer Life and Analytical Sciences, Boston, MA. [3H]PBR28 (61 Ci/ mmol) was acquired from Amersham, UK. In brief, to triplicate incubation tubes was added: 100 µL resuspended membranes; 100 µL radioligand; and 100 µL of either buffer (to measure total binding) or displacing agent. Nonspecific binding was defined as the residual in the presence of 3 µM PK 11195. The concentration of radioligand was ~ 0.40 nM for [3H]PBR28 and ~0.70 nM for [3H]PK 11195, which reflects the higher affinity of [3H]PBR28 compared to that of [3H]PK 11195. The protein concentration for the incubation was selected so that total bound (specific plus nonspecific) was < 10% of total added radioactivity. Thus, each tube contained ~ 1.5 µg protein for [3H]PBR28 and ~ 5 µg for [3H]PK 11195. Tubes were incubated for 30 min at room temperature. The reaction was terminated by filtration with a Brandel cell harvester (Gaithersburg, MD) through Whatman GF/A filter paper, followed by three washes of 1 mL ice-cold buffer. Because [3H]PK 11195 is highly lipophilic and has high adsorption to the filter paper, the filter papers were pretreated with 0.5% polyethyleneimine in buffer. Radioactivity in the individual circles of filter paper was measured with liquid scintillation counting for 5 min using 4 mL of Ultima-Gold fluid (Perkin Elmer, Chicago, IL). Since the concentration of

radioligand varied slightly between days, specific binding was linearly normalized to a single concentration: 0.50 nM for both radioligands.

To separately measure B_{max} and K_D, we displaced each radioligand with increasing concentrations of non-radioactive compound (from 100 pM to 3 µM). Data were analyzed using Scatchard homologous displacement with GraphPad Prism version 5.00 for Windows (GraphPad Software, San Diego, California, USA), which uses nonlinear fitting for homologous displacement. To measure K_I of PBR28 in binders and non-binders, we displaced [3H]PK 11195 with increasing concentrations of non-radioactive PBR28 (from 100 pM to 3 µM). To calculate K_I, $K_D = 4.7$ nM was used for binders and non-binders. Data were analyzed using one-site competitive binding with Graphpad Prism.

Monkey whole-body study

All animal experiments were performed in accordance with the Guide for the Care and Use of Laboratory Animals and were approved by the NIMH Animal Care and Use Committee. Two male rhesus monkeys (*Macaca mulatta*, 13.2 ± 2.1 kg) underwent baseline whole-body PET scans after intravenous injection of [11C]-(*R*)-PK 11195 (276 ± 8 MBq) via the posterior tibial vein. Following the baseline scan, the two monkeys underwent a second whole-body PET scan after blockade of TSPO by nonradioactive PBR28 (5 mg/kg i.v.). The blocking agent was administered 30 min before the injection of [11C]-(*R*)-PK 11195 (277 ± 21 MBq).

Animal preparation was identical to that previously described for whole-body studies using [11C]PBR28 (Brown et al., 2007; Imaizumi et al., 2008). 2D dynamic scans were acquired on the GE Advance tomograph in 4 segments of the body (head to upper thigh) in frames of increasing duration (75 s to 15 min) for a total scan time of 120 min (22 frames).

Images were analyzed using the methods described below for the human whole-body study. Organ uptake was also calculated as the area under the time-activity curve from 0 to 120 min, in order to compare with previously reported biodistribution data for 11C-PBR28 (Imaizumi et al., 2008).

Monkey brain study

Two male rhesus monkeys (8.6 ± 0.4 kg) underwent baseline brain PET scans after intravenous injection of [11C]-(*R*)-PK 11195 (187 ± 13 MBq) via the posterior tibial vein. Following the baseline scan, the two monkeys underwent a second brain PET scan after pre-blockade of TSPO by nonradioactive PBR28 (5 mg/kg i.v.). The blocking agent was administered two min before the injection of [11C]-(*R*)-PK 11195 (174 ± 37 MBq). Animal preparation was identical to that in the monkey whole-body scans. The PET scans were acquired in 3D dynamic mode using a GE Advance tomograph for a total scan time of 120 min (6×30 s, 3×1 min, 2×2 min, 22×5 min).

Blood samples (1 mL each) were drawn from the femoral artery at 15-s intervals until 120 s and again at 3 min, followed by 2-mL samples each at 5, 10, 30, 60, 90 and 120 min. Radioactivity in plasma was quantified by a γ-counter and analyzed by reverse-phase chromatography to separate parent radioligand from radiometabolites.

Total distribution volume, V_T, was measured at baseline and after receptor blockade using an unconstrained two-tissue compartment model and metabolite-corrected arterial input function. Specific distribution volume, V_S, was calculated as the difference of values of V_T at baseline and after receptor blockade.

Image analysis of both monkeys and humans used PMOD 2.95 software (PMOD Technologies, Zurich, Switzerland).

Substrate specificity of [³H]PK 11195 and of [³H]PBR28 at three ABC transporters

Three pairs of cell lines were used, each pair consisting of a parental (control) line and a resistant (ABC transporter expressing) line. The three pairs were (listed as parental and resistant, respectively): KB-3-1 and KB-8-5-11 (ABCB1, also called P-glycoprotein), H460 and H460/MX20 (ABCG2), and MCF-7 and MCF-7/VP16 (ABCC1). Cells were cultured as reported (Lee et al., 1998). KB and MCF-7 cell lines were cultured in Dulbecco's Modified Eagle's Medium, while H460 cell lines were cultured in Roswell Park Memorial Institute 1640 medium. Drug-resistant cell lines were additionally cultured in the following cytotoxic drugs to maintain ABC transporter expression: colchicine (100 ng/mL) for KB-8-5-11 (Shen et al., 1986), mitoxantrone (20 nM) for H460/MX20 (Henrich et al., 2007), and etoposide (4μM) for MCF-7/VP16 (Calcagno et al., 2006; Schneider et al., 1994). Chemicals for cell culture were purchased from Sigma-Aldrich (St. Louis, MO).

Accumulation of [³H]PK 11195 and [³H]PBR28 into cells expressing ABC transporters was determined by plating and incubating each cell line (2.5×10^5 cells/well) in 24-well plates for 24 h at 37 °C. To ensure stable accumulation of the radioligands, the time course of accumulation of each was measured in KB-3-1 cells at the following times in triplicate: 0, 5, 10, 20, 30, and 60 min. To initiate the assay, 5 nM of one radioligand was added to each well and the cells incubated at 37 °C. The radioactive media was then aspirated, and cells were washed with 500 µL of ice-cold 1x PBS and incubated with 100 µL trypsin for 90 min at 37 °C to ensure complete lysis. Radioactivity in cell lysates was assayed by liquid scintillation counting for 5 min using 10 mL of Bio-Safe II fluid (Research Products International Corp., Mount Prospect, IL). Cell counts were determined by counting the number of plated cells in three representative wells per plate using a Cellometer Automatic Cell Counter (Nexcelcom, Lawrence, MA). Non-specific binding to the plates was determined using cell-free wells. Experimental counts were corrected for non-specific binding, radioactivity was converted to femtomoles using the specific activity of [³H]PK 11195 and [³H]PBR28, and counts standardized to femtomoles per 1×10^6 cells.

To determine if [³H]PK 11195 and [³H]PBR28 were substrates of ABCB1 (P-glycoprotein), KB-3-1 and KB-8-5-11 cells were pre-incubated with 10 µM of the ABCB1 inhibitor cyclosporin A for 30 min at 37 °C before incubation with radioactivity. Following incubation for 30 min at 37°C, cells were washed, lysed, counted, and standardized as described above. Differences in means (from three observations) were analyzed for significance using the Student's *t-test* (unpaired, two-tailed, $\alpha = 0.05$).

RESULTS

Human whole-body imaging

Whole-body imaging was performed using both [¹¹C]-(*R*)-PK 11195 and [¹¹C]PBR28 to determine if [¹¹C]-(*R*)-PK 11195 distinguished human binders and non-binders. We closed the study once we determined that we had included five binders (two female, three male) and five non-binders (three female, two male). Non-binders were aged 27 ± 3 years and binders 39 ± 11 years. This difference in age was not statistically significant (p > 0.05, two-tailed t-test). One subject, a binder, was taking rosuvostatin and loratadine at the time of PET imaging. All other subjects were free of medications other than vitamins.

The whole-body PET scans were well-tolerated by all human subjects, with no significant change in heart rate, blood pressure, respiratory rate, temperature, or ECG. In one non-binder, the kidneys were not visualized in the [¹¹C]PBR28 scan. With this exception, organs that are known to express moderate to high levels of TSPO (namely brain, heart, lung, spleen, and kidney) were well-identified. Upon visual inspection, binders had higher organ uptake than

non-binders with both $[^{11}C]$-(R)-PK 11195 and $[^{11}C]$PBR28, although the differences were more obvious with $[^{11}C]$PBR28 (Fig 1).

Among the five organs with moderate to high expression of TSPO, $[^{11}C]$-(R)-PK 11195 showed significantly lower uptake (SUV • min) in non-binders than in binders in only heart (p = 0.002) and lung (p = 0.009) but not in other organs (Table 1). In addition, the washout of radioactivity in heart and lung of non-binders was faster than that of binders (Fig 2A and C). Non-binders had a trend toward decreased uptake in spleen; however, this difference did not reach statistical significance (p = 0.1012). Binders and non-binders showed no difference in uptake of $[^{11}C]$-(R)-PK 11195 in brain or kidney. The difference in uptake of heart and lung between binders and non-binders remained significant after correction for multiple comparisons using false discovery rate with five target organs.

In contrast to $[^{11}C]$-(R)-PK 11195, $[^{11}C]$PBR28 showed significantly lower uptake in non-binders than in binders in all five target organs (Table 1; p < 0.001). Uptake was lower in the non-binders at all time points, and washout of radioligand was accelerated in the non-binders. In each organ, the difference in uptake between binders and non-binders was greater with $[^{11}C]$PBR28 than with $[^{11}C]$-(R)-PK 11195 (Fig 2B and D).

In vitro binding to leukocyte membranes

Based on the results of the *in vivo* studies, we wondered if the phenomenon of non-binding was due to an absence of TSPO binding sites. In addition, we wished to perform *in vitro* displacement assays to look for supportive evidence of a shared binding site between PBR28 and PK 11195.

The specific binding of $[^3H]$PBR28 at a single radioligand concentration to leukocytes of the non-binders was negligible compared to that of the binders (Table 2). The specific binding of $[^3H]$PBR28 was 36-fold lower in eight non-binders than in ten binders. In contrast, the specific binding of $[^3H]$PK 11195 at a single radioligand concentration was similar for these two groups. To determine whether $[^3H]$PBR28 and $[^3H]$PK 11195 bind to distinct sites on TSPO, we displaced each radioligand by itself (homologous displacement) and by the compound (heterologous displacement). Measured at a single radioligand concentration, the specific binding of both radioligands was similar in the binders and non-binders using heterologous and homologous displacement (Table 2).

Unlike the negligible specific binding of $[^3H]$PBR28 in the non-binders, $[^3H]$PK 11195 had adequate signal in both groups to separately measure B_{max} and K_D with a saturation assay using homologous displacement by nonradioactive PK 11195. We found that the B_{max} and K_D of $[^3H]$PK 11195 were similar between binders and non-binders (Table 2).

We wished to do heterologous displacement in leukocyte membranes from non-binders but could do so only with $[^3H]$PK 11195, since $[^3H]$PBR28 has negligible binding in this group. The K_I of PBR28 was higher in non-binders (67 ± 38, range 39 – 140) than in binders (6.1 ± 6.4, range 0.30 – 17) (Table 2).

Taken together, these binding data show that PK 11195 and PBR28 bind to the same site, but that PBR28 has 10-fold lower affinity for TSPOs in non-binders compared to that in binders.

Monkey whole-body imaging

Previous studies using $[^{11}C]$-(R)-PK 11195 have not reported the existence of non-binders, and we were unable to distinguish binders and non-binders in the brain using this radioligand. We wondered if the reason that $[^{11}C]$-(R)-PK 11195 does not detect non-binders in the brain was

due to a low ratio of specific to non-specific binding in the brain, compared to peripheral organs in which $[^{11}C]$-(R)-PK 11195 did distinguish binders and non-binders (heart and lung).

Pre-blockade with nonradioactive PBR28 reduced overall uptake of $[^{11}C]$-(R)-PK 11195 in brain, heart, lung, spleen, and kidney (Fig 3). For the peripheral organs, the area under the time-activity curve (SUV • min) from 5 to 20 min was 38 – 76% lower in the pre-blocked scans than in the baseline scans (heart, 75.1 *vs*. 33.6; lung, 29.6 *vs*. 18.3; spleen, 87.1 *vs*. 20.6; kidney, 166.3 *vs*. 60.5).

Pre-blockade accelerated washout of radioactivity from brain, but less dramatically than from some peripheral target organs. Brain uptake declined to 50% of peak at 30 minutes, whereas other organs declined to 50% of peak within only 5 minutes. For this reason, the area under the brain time-activity curve from 5 to 20 min was similar for both the baseline and pre-blocked scans (28.2 *vs*. 29.1 SUV • min). Thus pre-blockade of TSPO has a less dramatic effect on $[^{11}C]$-(R)-PK 11195 binding in the brain than in the measured peripheral organs.

We also calculated the area under the time-activity curve from 0 to 120 minutes to compare specific organ uptake of $[^{11}C]$-(R)-PK 11195 to that reported using $[^{11}C]$PBR28. Using $[^{11}C]$-(R)-PK 11195, pre-blockade with nonradioactive PBR28 decreased the area under the curve by only 31%, 14%, and 30% in lung, brain, and kidney, respectively. Using $[^{11}C]$PBR28, pharmacological blockade was previously reported to decreased the area under the curve by 70%, 42%, and 50% in lung, brain, and kidney, respectively (Imaizumi et al., 2008).

Monkey brain imaging

To more accurately quantify the amount of specific binding of ^{11}C-(R)-PK 11195 in the monkey brain, we performed dedicated brain imaging. The specific binding of $[^{11}C]$-(R)-PK 11195 in monkey brain was measured at baseline and after blockade of TSPO with non-radioactive PBR28. The peak uptake of radioactivity in monkey brain after blockade (3.43 SUV) was higher than that in the baseline condition (1.64 SUV) (Fig 4A). The peak plasma concentration of $[^{11}C]$-(R)-PK 11195 after blockade (23.4 SUV) was also higher than that in the baseline condition (8.82 SUV) (Fig 4B). We found similar results with $[^{11}C]$PBR28 in monkey brain, and this effect was caused by displacement of TSPOs in the periphery, causing higher concentrations of radioligand in plasma, and thereby driving more radioactivity into brain.

Since pre-blockade caused changes in the concentration of radioligand in plasma, we performed compartmental analysis using the metabolite-corrected arterial input function. This measurement corrects differences of arterial input between scans.

Total binding of $[^{11}C]$-(R)-PK 11195, measured by compartmental modeling and defined as the total distribution volume (V_T; mL • cm^{-3}), was 49 – 64% lower after pre-blockade than at baseline (Table 3). Specific binding (V_S; mL • cm^{-3}), calculated as the difference in V_T at baseline and blocked conditions, was 1.22 in the cerebellum, 3.12 in the occipital cortex, 2.33 in the frontal cortex, and 1.17 in the parietal cortex. The average value of V_S in these four regions was 1.96 mL • cm^{-3}. The amount of specific binding we calculated in the monkey cerebellum (1.22 mL • cm^{-3}) was about 80-fold lower than the V_S reported for this region using $[^{11}C]$PBR28 (95.5 mL • cm^{-3}), which was also measured in rhesus monkey brain before and after pharmacological blockade (Imaizumi et al., 2008).

Substrate specificity of $[^3H]$PK 11195 and of $[^3H]$PBR28 for three ABC transporters

The 80-fold difference in specific binding between $[^{11}C]$-(R)-PK 11195 and $[^{11}C]$PBR28 was unexpected, and we wondered if the low amount of specific binding of $[^{11}C]$-(R)-PK 11195 was caused by an ABC transporter at the blood-brain barrier preventing uptake of this

radioligand. To answer this question, we measured the substrate specificity of $[^3H]PK$ 11195 and $[^3H]PBR8$ for the three major ABC transporters at the blood brain barrier: ABCB1 (P-glycoprotein), ABCC1, and ABCG2. Substrate specificity was determined by measuring the accumulation of radioactivity in three pairs of cell lines, where one cell line from each pair selectively over-expressed ABCB1, ABCC1, or ABCG2. To be a substrate for a transporter, uptake of the radioligand must be different between the two cell lines that make up a pair AND this difference must be blocked by a selective inhibitor of the transporter. Based on these two criteria, we found that neither $[^3H]PK$ 11195 nor $[^3H]PBR8$ was a substrate for these three transporters. Uptake of both radioligands was similar in the pairs of cell lines that express ABCC1 and ABCG2 (Supplemental Table 1). Although both radioligands showed higher uptake in parental than ABCB1 overexpressing cells, this difference was not blocked by the selective ABCB1 inhibitor cyclosporin A (Supplemental Table 1). Thus, inhibition of ABCB1 (P-glycoprotein) did not increase accumulation of either radioligand into ABCC1 over-expressing cells.

DISCUSSION

In this study, we sought to answer two questions: 1) What is the cause of non-binding to $[^{11}C]$ PBR28? and 2) Why has this phenomenon not previously been reported using $[^{11}C]$-(R)-PK 11195? With caveats that are discussed later, we found that non-binding is caused by the TSPO protein in non-binders having 10-fold lower affinity for PBR28 than the TSPO protein in binders. In addition, this phenomenon may have been overlooked because $[^{11}C]$-(R)-PK 11195 has very low specific signal in brain. These findings are based on four different experiments. First, to determine whether non-binding is unique to $[^{11}C]$PBR28, we scanned five binders and five non-binders with both radioligands: $[^{11}C]$PBR28 and $[^{11}C]$-(R)-PK 11195. We found that non-binders identified with $[^{11}C]$PBR28 also had significantly reduced binding in peripheral organs with high density of TSPO (lung and kidney) but not in brain. Thus, non-binding, at least in peripheral organs, appears to have been overlooked with $[^{11}C]$-(R)-PK 11195. Second, to determine whether non-binding could be caused by a lack of expression of the TSPO protein, we measured *in vitro* binding of $[^3H]PK$ 11195 and $[^3H]PBR28$ to cell membranes of peripheral leukocytes. We found that the binding of $[^3H]PK$ 11195 was equivalent in both groups, but the binding of $[^3H]PBR28$ was decreased 36-fold in non-binders compared to that in binders. The decreased binding was caused by decreased affinity of PBR28 (but not of PK 11195) to TSPO in leukocytes of non-binders. Thus, non-binders do express the TSPO protein at least in leukocytes (detected by binding of $[^3H]PK$ 11195), but the affinity of this protein for PBR28 is reduced greater than 10-fold. Third, the phenomenon of non-binding may have been overlooked with $[^{11}C]$-(R)-PK 11195 because this radioligand has a low ratio of specific to nonspecific binding in brain. To accurately measure the percentage specific binding in monkey brain, we obtained both PET brain and plasma data in monkeys, at baseline and after receptor-saturating doses of nonradioactive TSPO ligand. We found that the specific binding of $[^{11}C]$-(R)-PK 11195 in monkey cerebellum is about 80-fold lower than that of $[^{11}C]$PBR28. In addition, whole body imaging showed that specific (displaceable) binding of $[^{11}C]$-(R)-PK 11195 in peripheral organs was also less than that for $[^{11}C]$PBR28. Thus, the phenomenon of non-binding may have been overlooked with $[^{11}C]$-(R)-PK 11195 because of its low specific signal. Fourth, the phenomenon of non-binding might be caused by efflux transporters (including P-gp) at the blood-brain barrier that block the entry of the radioligand. Using human cells that specifically over-express each of the three most prevalent efflux transporters at the blood-brain barrier, we found that neither PK 11195 nor PBR28 is a substrate. Thus, blockade of entry into brain does not explain either non-binding to $[^{11}C]$PBR28 or the low specific binding of $[^{11}C]$-(R)-PK 11195.

In addition to the above determinations, based on results from our experiments, we also conclude that PBR28 and PK 11195 share a binding site on TSPO. We base this conclusion

on our *in vitro* results using membranes of human leukocytes, which showed that [³H]PBR28 and [³H]PK 11195 fully displace each other. Our conclusion is also supported by our *in vivo* monkey data showing that [¹¹C]-(*R*)-PK 11195 binding is displaced by nonradioactive PBR28. Imaizumi et al. (2008) previously demonstrated that [¹¹C]PBR28 binding in monkeys is displaced by nonradioactive PK 11195.

Questions raised by this study

Two major questions were raised by these studies. First, the differential uptake of [¹¹C]-(*R*)-PK 11195 and [¹¹C]PBR28 in target organs suggests that TSPOs vary among these organs, but we do not have direct evidence for such variation. Many studies have reported that drug selectivity of binding to TSPO varies among species and that the density of TSPOs varies among organs of the same species. For example, the original name of TSPO, "peripheral benzodiazepine receptor," derives from the fact that benzodiazepines like diazepam have high affinity for TSPO in rat, but subsequent studies showed much lower affinity of these agents at human TSPO (Papadopoulos et al., 2006). In addition, some target organs, especially lung and kidney, tend to have higher densities of binding sites than others. However, organs within a single species are thought to have the same TSPO protein with the same drug selectivity (Veenman et al., 2007). Our imaging results question this dogma, at least in the non-binders. That is, our results suggest that the TSPOs in heart and lung of non-binders have different drug selectivity (PK 11195 vs. PBR28) than those in brain, spleen, and kidney. We hope in the future to obtain postmortem tissues from binders and non-binders to test this suggestion with *in vitro* binding of [³H]PK 11195 and [³H]PBR28.

The uptake of [¹¹C]-(*R*)-PK 11195 was different between binders and non-binders in only two of the five target organs, but specific binding in some organs may have been obscured by the high nonspecific binding of [¹¹C]-(*R*)-PK 11195. For example, monkey brain imaging showed that the ratio of nonspecific to specific binding of [¹¹C]-(*R*)-PK 11195 was much greater than that for [¹¹C]PBR28. If the same is true for human brain, the high non-specific binding of [¹¹C]-(*R*)-PK 11195 may have obscured real differences of specific binding in binders compared to non-binders.

The second major question raised by this study is what physicochemical properties of PK 11195 and PBR28 allow one but not the other to distinguish binders from non-binders (e.g., under *in vitro* conditions) and whether these physicochemical properties also affect the binding of other radioligands for TSPO. We do not know the answers to these questions but plan additional binding studies in tissues from binders and non-binders using a variety of ligands with varying physicochemical properties.

Specific binding is different under in vivo and in vitro conditions

The imaging studies in monkeys demonstrated that the *in vivo* specific binding of [¹¹C]-(*R*)-PK 11195 is much lower than that of [¹¹C]PBR28. For monkeys, we could pharmacologically block the receptors and thereby measure specific binding as the difference between baseline and blocked conditions. For the monkey brain, but not peripheral organs, we also corrected for higher exposure from radioligand in plasma, which was caused by blockade of TSPOs in the periphery. This fully quantified measure of specific binding (V_S) for [¹¹C]-(*R*)-PK 11195 was 80-fold lower than that done previously in our laboratory for [¹¹C]PBR28 (Imaizumi et al., 2008). We do not feel that the lower amount of specific binding of [¹¹C]-(*R*)-PK 11195 was caused by differences in specific activity between the two radioligands. Although the specific activity of [¹¹C]-(*R*)-PK 11195 in the monkey brain study (101 ± 18 GBq/µmol) was lower than that reported for [¹¹C]PBR28 (229 ± 16 GBq/µmol), this 2-fold difference does not explain the 80-fold difference in specific binding.

Although the imaging studies demonstrated higher specific binding of [^{11}C]PBR28 compared to [^{11}C]-(*R*)-PK 11195, the *in vitro* experiments do not explain the magnitude of the differences. Under tracer conditions of radioligand imaging, specific binding equals the product of receptor density and affinity, with the latter inversely proportional to K_D (Innis et al., 2007). In the current study, the K_D of racemic [^{3}H]PK 11195 was only about two-fold higher than that of [^{3}H]PBR28 (Table 2). This difference would likely be negligible for the more active *R*-enantiomer used for PET imaging.

The difference of specific binding in monkey for [^{11}C]PBR28 and [^{11}C]-(*R*)-PK 11195 is also not explained by *in vitro* affinity. The K_I of PBR28 to monkey brain is 0.94 nM (Briard et al., 2008), whereas that of PK 11195 is 4.35 nM. This 4-fold difference of affinity does not fully explain the 80-fold difference in *V*s found in this study, even with correction for use of the *R*-enantiomer in PET.

We considered the possibility of P-glycoprotein or another ABC transporter limiting brain entry of [^{11}C]-(*R*)-PK 11195 as another possible explanation for the difference of specific binding in monkey for [^{11}C]PBR28 and [^{11}C]-(*R*)-PK 11195. However, we determined that neither radioligands are substrates for ABCB1, ABCG2, or ABCC1. Therefore, preferential efflux of [^{11}C]-(*R*)-PK 11195 at the blood-brain barrier is not the reason for decreased specific binding of this radioligand.

Discrepancies between *in vivo* and *in vitro* conditions commonly occur and can be caused by different experimental environments – e.g., temperature, fluid composition, and presence of intact mitochondria. This last possibility may be particularly important for TSPO, which forms a complex in the outer mitochondrial membrane with two other proteins: an adenine nucleotide transporter and a voltage-dependent anion channel (Papadopoulos et al., 2006). This trimeric protein complex may well be disrupted during homogenization of the leukocytes.

Cause of non-binding found with [^{11}C]PBR28

We now know that the cause of non-binding of [^{11}C]PBR28 in about 10% of subjects is its low affinity for TSPO. The next logical question is how TSPOs differ between binders and non-binders. We are now pursuing potential genetic markers of this difference. In addition to several polymorphisms, TSPO is reported to have alternate mRNA splicing of exon 2, which is thought to contain the binding site for [^{3}H]PK 11195 (Lin et al., 1993; Zhang et al., 2006). Furthermore, this alternate splicing may be variably expressed in organs of the body.

CONCLUSION

Based on binding of [^{3}H]PK 11195 to leukocyte membranes, both binders and non-binders express TSPO. Based on comparable studies using [^{3}H]PBR28, non-binding to PBR28 is caused by its low affinity for TSPO in non-binders. Whole body imaging with the ^{11}C-labeled radioligands showed that [^{11}C]PBR28 detects non-binding in all five target organs with high densities of TSPO (lung, heart, brain, kidney, and spleen). In contrast, [^{11}C]-(*R*)-PK 11195 detected non-binding in only heart and lung, which suggests that non-binding may be differentially expressed in organs of the body. Using fully quantitative studies with an arterial input function, the specific binding of [^{11}C]-(*R*)-PK 11195 in monkey brain was ~ 80-fold lower than that of [^{11}C]PBR28. Whole body imaging in monkeys showed that [^{11}C]-(*R*)-PK 11195 also has lower specific (displaceable) binding in peripheral organs than does [^{11}C]PBR28. The relatively low *in vivo* specific binding of [^{11}C]-(*R*)-PK 11195 may have obscured its detection of non-binding in peripheral organs. Finally, using human cells that specifically over-express each of the three most prevalent efflux transporters at the blood-brain barrier, we found that neither PBR28 nor PK 11195 is a substrate. Thus, blockade of entry into brain does

not explain either non-binding to [11C]PBR28 or the low specific binding of [11C]-(*R*)-PK 11195.

Supplementary Material

Refer to Web version on PubMed Central for supplementary material.

Acknowledgments

REFERENCES

Benjamin Y, Hochberg Y. Controlling the false discovery rate: a practical and powerful approach to multiple testing. J R Statist Soc B 1995;57:289–300.

Briard E, Zoghbi SS, Imaizumi M, Gourley JP, Shetty HU, Hong J, Cropley V, Fujita M, Innis RB, Pike VW. Synthesis and evaluation in monkey of two sensitive 11C-labeled aryloxyanilide ligands for imaging brain peripheral benzodiazepine receptors in vivo. J Med Chem 2008;51:17–30. [PubMed: 18067245]

Brown AK, Fujita M, Fujimura Y, Liow JS, Stabin M, Ryu YH, Imaizumi M, Hong J, Pike VW, Innis RB. Radiation dosimetry and biodistribution in monkey and man of [11C]PBR28: a PET radioligand to image inflammation. J Nucl Med 2007;48:2072–2079. [PubMed: 18006619]

Cagnin A, Kassiou M, Meikle SR, Banati RB. Positron emission tomography imaging of neuroinflammation. Neurotherapeutics 2007;4:443–452. [PubMed: 17599710]

Calcagno AM, Chewning KJ, Wu CP, Ambudkar SV. Plasma membrane calcium ATPase (PMCA4): a housekeeper for RT-PCR relative quantification of polytopic membrane proteins. BMC Mol Biol 2006;7:29. [PubMed: 16978418]

Ferrarese C, Appollonio I, Frigo M, Perego M, Piolti R, Trabucchi M, Frattola L. Decreased density of benzodiazepine receptors in lymphocytes of anxious patients: reversal after chronic diazepam treatment. Acta Psychiatr Scand 1990;82:169–173. [PubMed: 2173354]

Fujita M, Imaizumi M, Zoghbi SS, Fujimura Y, Farris AG, Suhara T, Hong J, Pike VW, Innis RB. Kinetic analysis in healthy humans of a novel positron emission tomography radioligand to image the peripheral benzodiazepine receptor, a potential biomarker for inflammation. Neuroimage 2008;40:43–52. [PubMed: 18093844]

Henrich CJ, Robey RW, Bokesch HR, Bates SE, Shukla S, Ambudkar SV, Dean M, McMahon JB. New inhibitors of ABCG2 identified by high-throughput screening. Mol Cancer Ther 2007;6:3271–3278. [PubMed: 18089721]

Imaizumi M, Briard E, Zoghbi SS, Gourley JP, Hong J, Fujimura Y, Pike VW, Innis RB, Fujita M. Brain and whole-body imaging in nonhuman primates of [11C]PBR28, a promising PET radioligand for peripheral benzodiazepine receptors. Neuroimage 2008;39:1289–1298. [PubMed: 18024084]

Innis RB, Cunningham VJ, Delforge J, Fujita M, Gjedde A, Gunn RN, Holden J, Houle S, Huang SC, Ichise M, Iida H, Ito H, Kimura Y, Koeppe RA, Knudsen GM, Knuuti J, Lammertsma AA, Laruelle

M, Logan J, Maguire RP, Mintun MA, Morris ED, Parsey R, Price JC, Slifstein M, Sossi V, Suhara T, Votaw JR, Wong DF, Carson RE. Consensus nomenclature for in vivo imaging of reversibly binding radioligands. J Cereb Blood Flow Metab 2007;27:1533–1539. [PubMed: 17519979]

Lee CG, Gottesman MM, Cardarelli CO, Ramachandra M, Jeang KT, Ambudkar SV, Pastan I, Dey S. HIV-1 protease inhibitors are substrates for the MDR1 multidrug transporter. Biochemistry 1998;37:3594–3601. [PubMed: 9530286]

Lin D, Chang YJ, Strauss JF, Miller WL 3rd. The human peripheral benzodiazepine receptor gene: cloning and characterization of alternative splicing in normal tissues and in a patient with congenital lipoid adrenal hyperplasia. Genomics 1993;18:643–650. [PubMed: 8307574]

Moingeon P, Dessaux JJ, Fellous R, Alberici GF, Bidart JM, Motte P, Bohuon C. Benzodiazepine receptors on human blood platelets. Life Sci 1984;35:2003–2009. [PubMed: 6092810]

Papadopoulos V, Baraldi M, Guilarte TR, Knudsen TB, Lacapere JJ, Lindemann P, Norenberg MD, Nutt D, Weizman A, Zhang MR, Gavish M. Translocator protein (18kDa): new nomenclature for the peripheral-type benzodiazepine receptor based on its structure and molecular function. Trends Pharmacol Sci 2006;27:402–409. [PubMed: 16822554]

Petit-Taboue MC, Baron JC, Barre L, Travere JM, Speckel D, Camsonne R, MacKenzie ET. Brain kinetics and specific binding of [^{11}C]PK 11195 to omega 3 sites in baboons: positron emission tomography study. Eur J Pharmacol 1991;200:347–351. [PubMed: 1782994]

Schneider E, Horton JK, Yang CH, Nakagawa M, Cowan KH. Multidrug resistance-associated protein gene overexpression and reduced drug sensitivity of topoisomerase II in a human breast carcinoma MCF7 cell line selected for etoposide resistance. Cancer Res 1994;54:152–158. [PubMed: 7903202]

Shen DW, Cardarelli C, Hwang J, Cornwell M, Richert N, Ishii S, Pastan I, Gottesman MM. Multiple drug-resistant human KB carcinoma cells independently selected for high-level resistance to colchicine, adriamycin, or vinblastine show changes in expression of specific proteins. J Biol Chem 1986;261:7762–7770. [PubMed: 3711108]

Veenman L, Papadopoulos V, Gavish M. Channel-like functions of the 18-kDa translocator protein (TSPO): regulation of apoptosis and steroidogenesis as part of the host-defense response. Curr Pharm Des 2007;13:2385–2405. [PubMed: 17692008]

Zhang K, Demeure O, Belliard A, Goujon JM, Favreau F, Desurmont T, Mauco G, Barriere M, Carretier M, Milan D, Papadopoulos V, Hauet T. Cloning, sequencing, and chromosomal localization of pig peripheral benzodiazepine receptor: three different forms produced by alternative splicing. Mamm Genome 2006;17:1050–1062. [PubMed: 17019653]
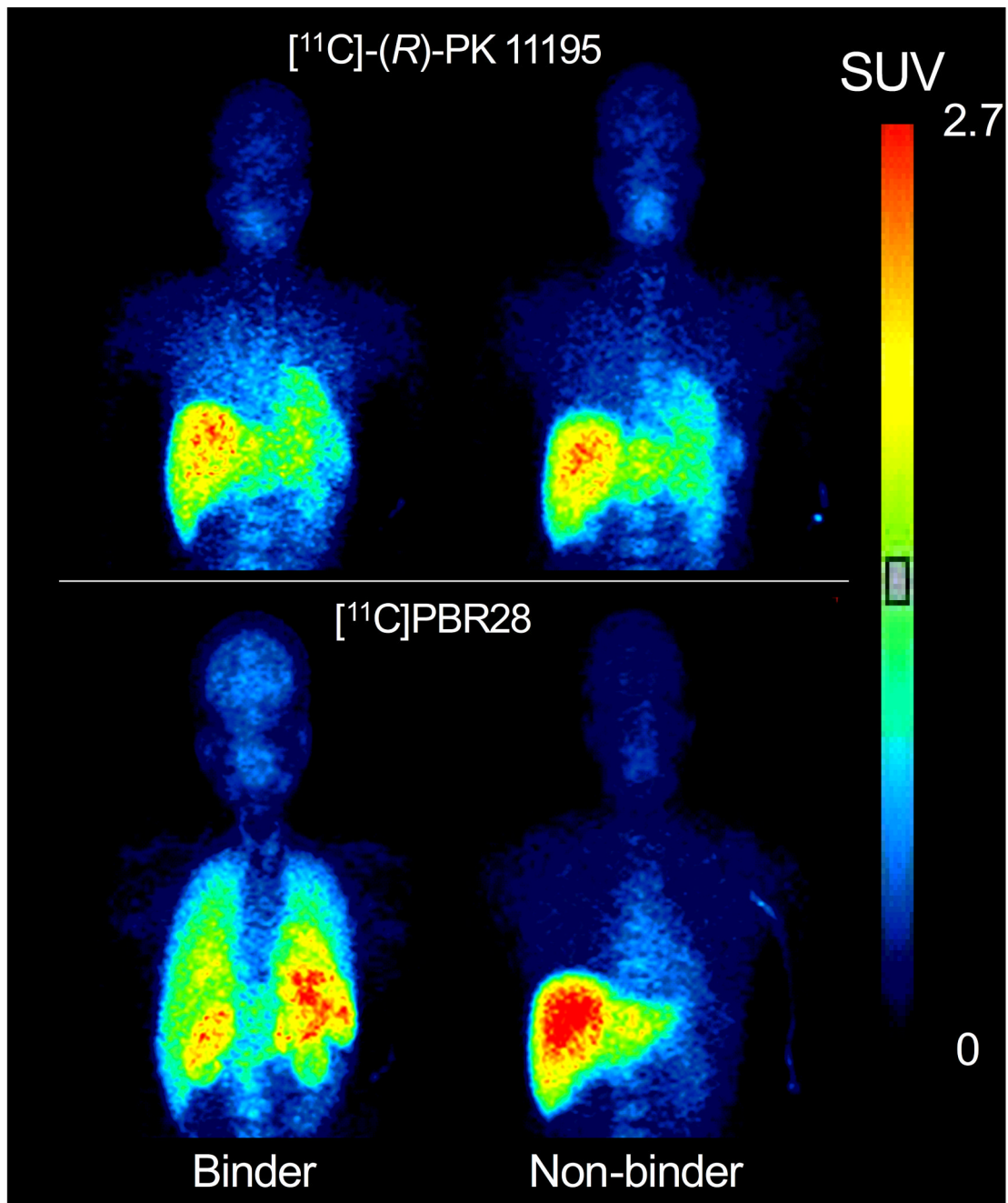
Figure 1.
Human whole body images from one binder (left) and one non-binder (right). Subjects were scanned with both $[^{11}C]$-(R)-PK 11195 (top) and $[^{11}C]$PBR28 (bottom). Images were obtained 10 min after injection of radioligand. Color bars represent concentration of radioactivity corrected for body weight and injected dose of activity (standardized uptake values). Note that these values are underestimated since displayed images are averaged in the anterior-posterior dimension.
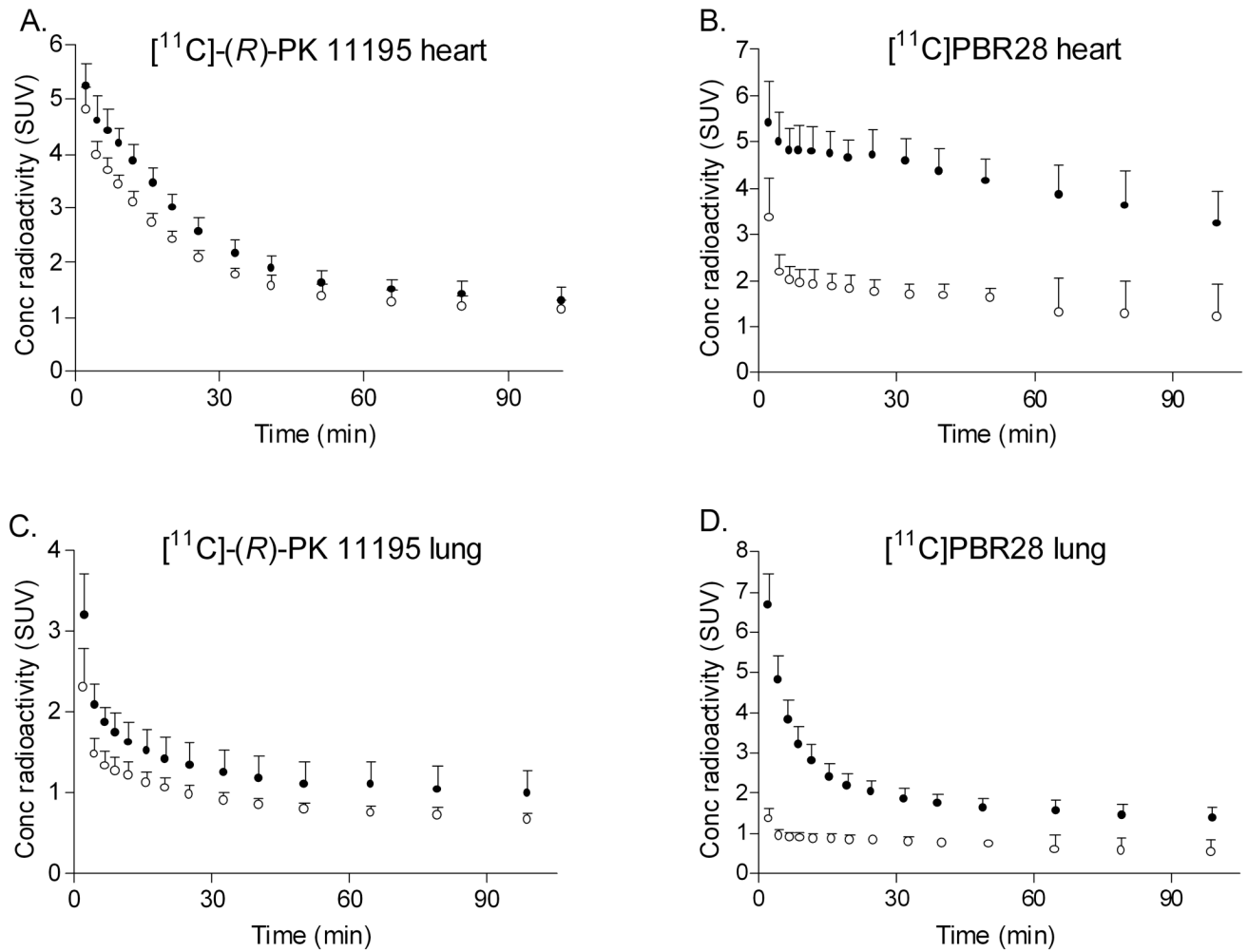
Figure 2.
Human time-activity curves for heart for [^{11}C]-(*R*)-PK 11195 (A) and [^{11}C]PBR28 (B), and for lung for [^{11}C]-(*R*)-PK 11195 (C) and [^{11}C]PBR28 (D). For each radioligand, (•) denotes binders and (○) denotes non-binders. Error bars denote standard deviation.

A.

B.
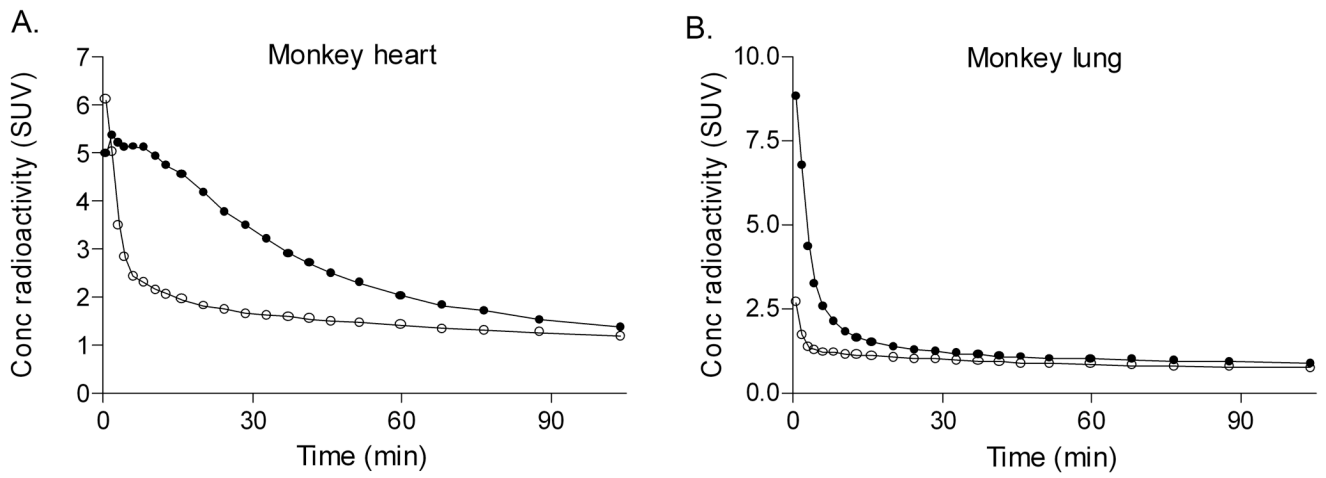
Figure 3.
Time-activity curves for heart (A) and lung (B) for two rhesus monkeys using $[^{11}C]$-(R)-PK 11195 at baseline (•) and after pre-blockade with 5 mg/kg nonradioactive PBR28 (○). For clarity, error bars are not shown. Conc = concentration.
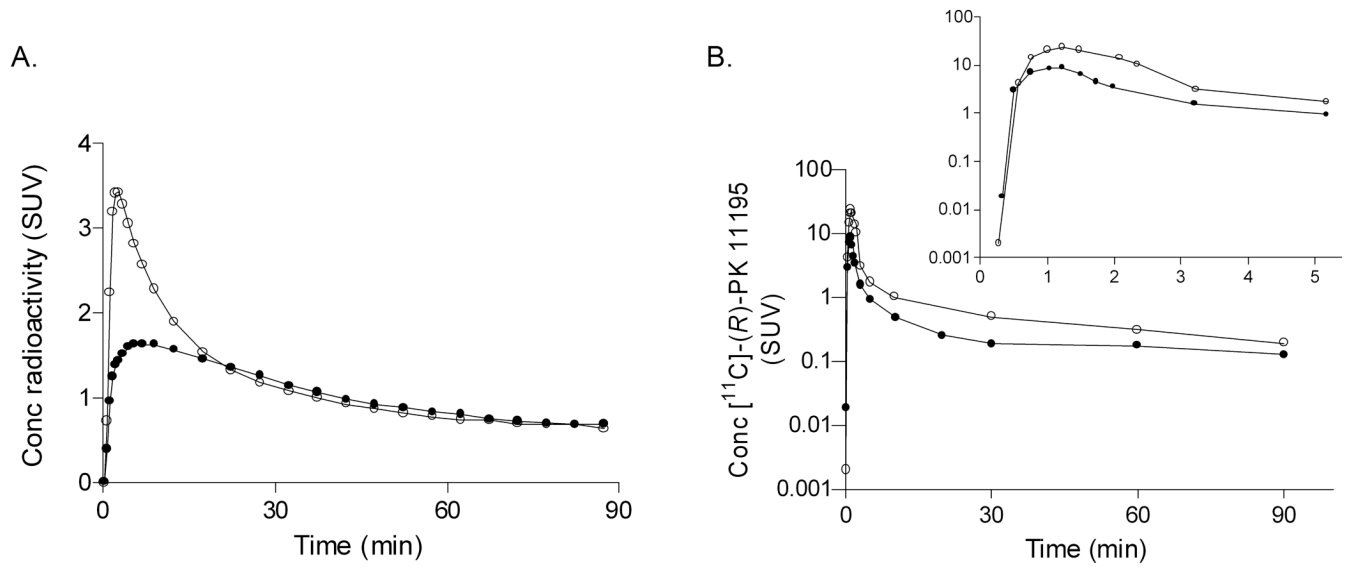
Figure 4.
A. Brain time-activity curves for a rhesus monkey using [^{11}C]-(*R*)-PK 11195 at baseline (•) and after pre-blockade with 5 mg/kg nonradioactive PBR28 (○). B. Plasma concentration of [^{11}C]-(*R*)-PK 11195 at baseline (•) and after pre-blockade with nonradioactive PBR28 (○). Insert: Plasma concentration curve magnified to demonstrate peak concentrations in plasma in both baseline and pre-blocked conditions.

TABLE 1

Organ uptake of $[^{11}C]$-(R)-PK 11195 and $[^{11}C]$PBR28 for human binders and non-binders.

	$[^{11}C]$-(R)-PK 11195 Organ uptake (SUV • min)		$[^{11}C]$PBR28 Organ uptake (SUV • min)	
Organ	Binders (n = 5)	Non-binders (n = 5)	Binders (n = 5)	Non-binders (n = 5)
Brain	18.8 ± 1.0	17.5 ± 2.0	27.3 ± 3.4	13.8 ± 1.3 [‡]
Lung	25.6 ± 3.7	18.7 ± 2.5 [*]	44.9 ± 6.5	13.6 ± 2.0 [‡]
Heart	59.8 ± 4.9	48.8 ± 2.8 [†]	72.3 ± 10.3	29.7 ± 4.7 [‡]
Spleen	65.6 ± 9.3	53.4 ± 11.4	131.6 ± 19.3	34.1 ± 11.0 [‡]
Kidney	63.8 ± 3.2	60.7 ± 12.3	109.3 ± 12.9	33.4 ± 15.5 [‡]

Data given as mean ± SD.

[*] p = 0.009,

[†] p = 0.002,

[‡] p < 0.001 vs. binders.

Table 2

Radioligand binding to membranes of leukocytes isolated from human binders and non-binders

Assay Type	Radioligand	Parameter	Displacer	Binders	Non-Binders
Single Radioligand Concentration	[³H]PK 11195	Specific Binding* (pmol / mg protein)	PK 11195	1.4 ± 0.4 (n = 10)	1.7 ± 0.8 (n = 8)
			PBR28	1.3 ± 0.5 (n = 10)	1.5 ± 0.8 (n = 8)
	[³H]PBR28	Specific Binding* (pmol / mg protein)	PBR28	7.2 ± 2.2 (n = 10)	0.2 ± 0.1 (n = 8)
			PK 11195	7.3 ± 2.2 (n = 10)	0.3 ± 0.1 (n = 8)
Saturation Curve	[³H]PK 11195	B_{max} (pmol / mg protein)	PK 11195	10.4 ± 7.1 (n=10)	15.1 ± 12.0 (n=8)
		K_D (nM)		4.7 ± 3.3 [†] (n = 10)	4.7 ± 2.3 (n = 8)
	[³H]PBR28	B_{max} (pmol / mg protein)	PBR28	16.9 ± 8.0 (n = 9)	ND
		K_D (nM)		1.8 ± 0.6 (n = 9)	ND
Displacement	[³H]PK 11195	K_i of PBR28 (nM)	PBR28	6.1 ± 6.4[‡] (n = 9)	67.4 ± 37.8 (n=8)

The entire sample size is described in Methods, but some samples were depleted during the course of this study.

Data are mean ± SD, with the sample size (n) listed below each value.

ND = not determined because specific binding was too low to measure accurately.

*
Specific binding was linearly normalized to a single radioligand concentration: 0.5 nM for both ligands.

[†] $p = 0.0129$ *vs.* [³H]PBR28,

[‡] $p = 0.0002$ *vs.* non-binders.

TABLE 3

$[^{11}C]$-(R)-PK 11195 binding (V_T) in two rhesus monkeys at baseline and after pre-blockade with nonradioactive PBR28.

Region	V_T (mL • cm^{-3})		
	Baseline	**Blocked**	**% change**
Cerebellum	2.60	1.38	−45
Occipital cortex	4.56	1.44	−64
Frontal cortex	3.82	1.49	−61
Parietal cortex	2.82	1.65	−40

Nonradioactive PBR28 (5 mg/kg i.v.) was injected 2 minutes prior to $[^{11}C]$-(R)-PK 11195